CORA Cork Open Research Archive
Cartlann Taighde Oscailte Chorcaí

Title	Highly mismatched III–V semiconductor alloys applied in multiple quantum well photovoltaics
Authors	Xiong, Wanshu;Broderick, Christopher A.;Rorison, Judy M.
Publication date	2018-01-15
Original Citation	Xiong, W., Broderick, C. A. and Rorison, J. M. (2018) 'Highly mismatched III–V semiconductor alloys applied in multiple quantum well photovoltaics', IET Optoelectronics, 12(1), pp. 15-19. doi: 10.1049/iet-opt.2017.0091
Rights	© 2017, Institution of Engineering and Technology. All rights reserved.
Download date	2026-11-06 18:34:05
Item downloaded from	https://hdl.handle.net/10468/5619

UCC
University College Cork, Ireland
Coláiste na hOllscoile Corcaigh

Highly Mismatched III-V Semiconductor Alloys Applied in Multiple Quantum Well Photovoltaics

Wanshu Xiong[1], Christopher A. Broderick[1,2], and Judy M. Rorison[1]
[1]*Department of Electrical and Electronic Engineering, University of Bristol, Bristol BS8 1UB, U.K.*
[2]*Photonics Theory Group, Tyndall National Institute, Dyke Parade, Cork T12 R5CP, Ireland*

Abstract

Adding dilute concentrations of nitrogen (N) or bismuth (Bi) into conventional III-V semiconductor alloys causes a large energy bowing of the bandgap due to modification of the electronic band structure. This behaviour has attracted significant interest due to the resulting optical and electronic properties. Firstly, we present the theoretical band structure models for GaAs-based dilute nitride, dilute bismide and dilute bismide-nitride alloys and then use this within current continuity equations to develop the photovoltaic behaviour. To describe the band structures of these highly mismatched III-V semiconductor alloys, we introduce a 10-, 12- and 14-band $\mathrm{k}\cdot\mathrm{p}$ Hamiltonian for dilute nitride, dilute bismide and dilute bismide-nitride semiconductors, respectively [1]. We then use this approach to analyse GaBiAs multi-QW p-i-n structures for photovoltaic performance.

Through our theoretical analysis we can: (i) elucidate important trends in the properties and photovoltaic performance of GaBiAs QW structures, and (ii) comment generally on the suitability of GaBiAs alloys and heterostructures for applications in Multi-junction Solar Cells. In particular, we identify and quantify the limitations associated with current GaBiAs solar cells, and describe the improvements in performance that can be expected pending further development of this emerging class of devices.

1. Introduction

The electronic structure of III-V semiconductor alloys have been studied for a long time. The simplest way to study such alloys is the virtual crystal approximation (VCA) [2], in which the electronic properties of the random alloys are offered by the linear interpolation between the end-point material properties. This approximation has been proved perfectly applicable to conventional III-V alloys [3]. Most of the understanding of semiconductor alloy systems only have small differences in properties at the end-point of semiconductor materials, they are called “well-matched” alloys. However, we found that incorporating N and Bi at dilute concentrations causes distinctly effects on the material properties, these N- and Bi-contained material will have some

impurity-like behaviour. As the atomic number of nitride (bismuth) is much smaller (larger) than other group V elements significant differences in size and electronegativity between them and the group-V atoms they replace occur. Hence, dilute nitride and dilute bismide alloys are considered to be “highly mismatched” alloys (HMAs).

Nitrogen and Bismuth incorporation into III-V semiconductor alloys results in numerous effects: a strong bowing in the band structure, an increase in the electron and hole effective mass and a significant reduction of the electron and hole mobility. When the smaller but highly electronegative nitrogen atoms substitutes group V atoms in III-V compounds, it primarily affects the conduction band (CB) structure of the alloys into which it is incorporated. Bi incorporation mainly effects the valence band (VB) structure due to its significantly larger size and being more electropositive than the group V atoms in host material. Substitution of As by Bi not only causes a strong reduction in the band gap (E_g), like dilute nitrides does, but also brings a rapid increase in the spin-orbit-splitting energy (Δ_{SO}) with increasing Bi composition x.

According to calculation, the strong N-induced decreasing in bandgap is about up to 180 meV per percentage N at low nitrogen composition [4][5], and 1% of Bi into GaAs reduces the E_g by about 90 meV [6][7][8][9][10][11], as well as an increase of approximately 65 meV in the valence band spin-orbit splitting energy [10], all of which are characterised by strong, composition-dependent bowing. The highly engineerable band structure of dilute nitride, dilute bismide and dilute bismide-nitride alloys has stimulated ongoing activity to explore and exploit their potential for a range of practical applications, including in GaAs-based long-wavelength semiconductor lasers, spintronics, and photovoltaics.

The theoretical modelling of highly mismatched alloys is significantly complicated as the impurity-like behaviour of the N or Bi atoms when incorporating into host materials and causes a strong perturbation of the electronic band structure of the alloys. The band structures of these high mismatched alloys can be explained in terms of the Band Anti-Crossing (BAC) model [1] which was developed to describe the pressure and composition dependent bandgap behaviour of the HMAs. The band gap bowing in dilute nitride alloys has been well explained by a two-level BAC model. The anti-crossing interaction is between the highly localized state of the substitutional N atoms, and the extended CB edge states of the hose semiconductor matrix. Meanwhile for dilute bismide alloys, the BAC model is a valence band anti-crossing model (VBAC) and the interaction occurs between the Bi-related impurity levels and the valence band edge

states. We present a general formalism to deal with dilute nitride, dilute bismide and dilute bismide-nitride alloys. We then present a model to investigate the features of highly HMA systems which influence the absorption coefficient and internal quantum efficiency (IQE). The model is based on a general solution of the minority carrier equation [12]. IQE is an important parameter in the performance of the solar cells. An accurate IQE equation can illustrate the effects of diodes' parameters to the performance of the solar cells. Our model can be used to predict the IQE for HMA quantum well solar cells.

We will present the details for a series of GaBiAs quantum well (QW) solar cells as GaBiAs is a candidate to provide a suitable 1 eV junction for the development of highly efficient multiple junction solar cells (MJSCs). GaBiAs QWs solar cells have the potential to overcome key limitations associated with current approaches [13][14].

The paper's layout is as follows: In Sec. 2, we present details of the theoretical band structure models used to describe the HMAs and their role in calculating the absorption and internal quantum efficiency model. Sec. 3 contains the theoretical modelling results applied to the dilute bismide QW system. Sec. 4 draws conclusions on the models for highly mismatched alloys and discusses the p-i-n bismide QW photodiodes modelled showing the optimized structures.

2. Theoretical Model

2.1. Band Structure Model

It is well known that traditional III-V semiconductor material's band structure, like GaAs, can be well described by 8-band $\mathrm{k}\cdot\mathrm{p}$ model. However, incorporating N or Bi will cause a strong composition-dependent band gap bowing. Hence the 8-band model is no longer suitable for the highly-mismatch alloys, we have to introduce a new $\mathrm{k}\cdot\mathrm{p}$ model to describe the HMAs band structure which can well applicable to the simulation of the optical and electronic propertied of dilute nitride and dilute bismide materials. For dilute nitride alloys, as the incorporated N atoms mainly effects the CB of the host material, in the two levels conduction BAC model, the conduction band edge (CBE) energy of the N-contained alloys can be given by the lower eigenvalue of the 2-band Hamiltonian [1]:

$$H = \begin{bmatrix} E_N & V_{NC} \\ V_{NC} & E_{CB} \end{bmatrix}$$

where V_{NC} describes the interaction between the extended CB egde states at energy E_{CB} of the host material and the highly localised N-related impurity states at energ E_N. The interaction is dependent on the N composition y as $V_{NC} = \beta_N\sqrt{y}$.

As Bi atom is significantly larger than the host material atom (As), the Bi-related impurity levels usually lie below or close to the valence band (VB) edge in energy. Similar to the model of dilute nitride alloys, a valence band anticrossing (VBAC) interaction occurs between the impurity levels and the VB edge states. We can therefore derive a 12-band $\mathrm{k}\cdot\mathrm{p}$ Hamiltonian, present in full in [1], describes conduction (CB), heavy and light-hole (HH & LH), spin-split-o (SO) bands and four additional degenerate Bi-related states at energy E_{bi}. We use V_{Bi} to describe the interaction between the GaAs valence band edge (VBE) and the Bi-related impurity levels at energy E_{Bi}, and is taken to vary with Bi composition x as $V_{Bi} = \beta_{Bi}\sqrt{x}$. In this method, we calculate the energy of the Bi-related states, $E_{Bi} = \langle\psi_{Bi}|\hat{H}(x)|\psi_{Bi}\rangle$, and the coupling strength V_{Bi} premarily through the VBAC interaction between the impurity states and the host matrix valence band edge states.

Based on our previous study, we also find that the effects of N and Bi on the electronic structure of host matrix are largely independent of each other, both is ordered and disordered crystals . In additional, the interaction between the subsititutional N and Bi atoms in the supercells is smaller than 1 μeV [1], which means that the effects of N- and Bi-related impurity states on the electronic structure are decoupled. Therefore, the N- and B-related BAC interactions in the band structure of host matrix can be treated separately. Following this way, we can extend the 8-band basis set to 14-band model by directly adding the two additional degenerate N-related and four additional degenerate Bi-related states at energy E_N and E_{Bi}, respectively. In this manner, we are arrived at a 14-band $\mathrm{k}\cdot\mathrm{p}$ model for like $GaBi_xN_yAs_{1-x-y}$ dilute bismide-nitride alloys. In this model, the band structure of the N- and Bi-containing alloy also can be derived as the lower eigenvalue of the 7-band Hamiltonian:

$$H = \begin{bmatrix} E_N & V_{NC} & 0 & 0 & 0 & 0 & 0 \\ V_{NC} & E_{CB} & 0 & \sqrt{2}U & -U & 0 & 0 \\ 0 & 0 & E_{HH} & 0 & 0 & V_{Bi} & 0 \\ 0 & \sqrt{2}U^* & 0 & E_{LH} & Q & 0 & V_{Bi} \\ 0 & -U^* & 0 & Q^* & E_{SO} & 0 & 0 \\ 0 & 0 & V_{Bi}^* & 0 & 0 & E_{Bi}^{HH} & 0 \\ 0 & 0 & 0 & V_{Bi}^* & 0 & 0 & E_{Bi}^{LH} \end{bmatrix}$$

In this manner, all the incorporating N and Bi effects information have been taken into account, including the conduction and valence band energy shift due to the BAC, compressive or tensile strain due to the different size of N or Bi atoms and virtual crystal effects on the N or Bi composition dependence of the valence band edge energies.

Additionally, the 12-band model (shows inside of the right low black box of the 14-band $\mathrm{k}\cdot\mathrm{p}$ Hamiltonian) approach is capable of quantitatively describing the optical gain in GaBiAs/(Al)GaAs lasers structures and has already shown excellent agreement for those lasers structures [15]. The parameters we used in this work, such as virtual crystal contributions to CB, VB and SO band edge energies and Bi-related localised states related to the host material VB edge and the VBAC coupling strength can also be found in that reference. Therefore, the 12-band model can produce an extremely accurate description of the $GaBi_xAs_{1-x}$ band structure by comparing the theoretical calculated results with a range of experimental results from the literature.

2.2. Absorption and Internal Quantum Efficiency Model

The basic structure of our model is a GaAs p-i-n photodiode with a HMA QWs in the i-region. The layer diagram of the theoretical model here for the $GaBi_xAs_{1-x}$/GaAs multiple quantum well solar cells is shown in Fig.1.

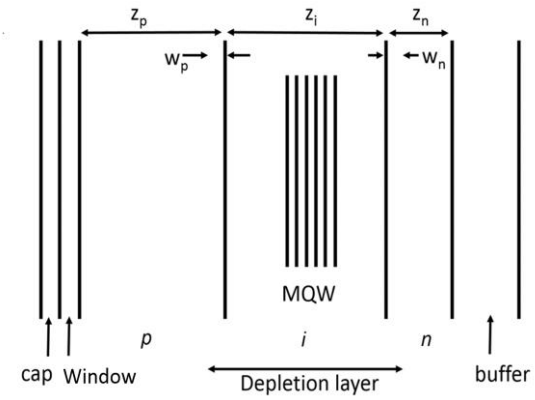


Fig. 1: Structure diagram of the model, showing optional the cap/window layer, the p-type, undoped MQW system in the i-region and n-type layers with respective widths z_p, z_i and z_n; w_n and w_p: depleted regions of the p and n layers.

When we implementate the $\mathrm{k}\cdot\mathrm{p}$ model to QWs solar cells, we used a standard absorption calculation by directly using the calculated QW eigenstates to compute the optical matrix element with an assumption that neglects the excitonic effects. The calculation of the absorption in the solar cells is similar to a gain calculation, but assumes that the valence (conduction) band is free of holes (electrons), and is called “free-carrier” absorption. We take this assumption

because when we considerate the N- or Bi-related alloy disorder on the states at the conduction or valence band edge in calculating the origin of the broad band edge features in the alloys, we find that the inhomogeneous broadening is much larger in magnitude compared to that in the conventional semiconductor alloys. Therefore, in terms of the absorption model used for these solar cell calculations, the broadening of the optical transitions is an input to the calculations. Based on the aforementioned band structure analysis, we found that in HMAs the inhomogeneous broadening of the optical transitions can be well described by using a hyperbolic secant lineshape function with an input linewidth. The large inhomogeneous broadening of the optical spectra is mainly caused by the N- or Bi-induced alloy disorder and the influence of clustering on the electronic stucture. In this work, the hyperbolic secant lineshape function for the inhomogeneous broadening is taken as:

$$S(\hbar\omega) = \frac{1}{\pi\delta} sech\left(\frac{E_0 - \hbar\omega}{\delta}\right)$$

where δ is the inhomogeneous broadening linewidth.

As we know, the internal quantum efficiency (IQE) spectrum reflects the cell design and the material quality. We calculate the model's internal quantum efficiency by solving the carrier transport equations in the minority carrier and depletion approximations at room temperature [12]. The assumptions of uniform doping, low injection and non-abrupt absorption coefficient are justified for these dilute bismide materials and enable an analytic solution of the carrier transport equations. Our model for the IQE of HMA multiple QWs solar cells are based on a general solution of the one-dimensional continuous function at room temperature. In a uniform fieldness p-type (n-type) layer, the excess electron (hole) concentration $n(z)$ ($p(z)$) at a point z satisfies:

$$D_{n,p} \frac{d^2 n, p(z)}{dz^2} - \frac{D_{n,p}}{l_{n,p}^2} n, p(z) + G(\lambda, z) = 0$$

where l_n (l_p) is the electron (hole) diffusion length and D_n (D_p) is the electron (hole) diffusion constant in p (n) region. And $G(\lambda, z)$ is the electron-hole-pair generation rate at a depth z beneath the surface:

$$G(\lambda, z) = F(\lambda)[1 - \mathrm{R}(\lambda)]\alpha(\lambda, z) exp\left(-\sum \alpha_i z_i\right) \exp(-\alpha_p z)$$

where $F(\lambda)$ is the flux function, $\mathrm{R}(\lambda)$ is the surface reflectivity, and $\alpha(\lambda, z)$ is the local absorption coefficient. Those equations above should follow the boundary conditions which the excess

electron and hole densities vanish at the edges of the depletion zone and the surface recombination absorbs the current at front and back surfaces with surface recombination velocities S_n and S_p, respectively. We calculate the diffusive photocurrent generated $J_{n,p}$ from the p and n region at the edges of the depletion zone and the contribution from the carriers photogenerated in the depletion region J_{dr}:

$$J_{n,p} = qD_{n,p}\frac{dn,p}{dz}$$

$$J_{dr} = qF(\lambda)[1-\mathrm{R}(\lambda)]\cdot exp\left(-\alpha_{cap}z_{cap}\right)\times\left(1-exp\left(-\alpha_p z_p-\alpha_i z_i-\alpha_n z_n\right)\right)$$

We make some assumptions here: (i) neglecting the contributions to the photocurrent from the optional cap and window layers. Because the cap layer will only slightly passivate the surface and cannot make any contribute to the photocurrent. And when the window layer is thin enough, the enhanced photocurrent at short wavelength due to the window layer can be well approximated using a reduced surface recombination velocity; (ii) assuming that intrinsic region free of traps, the built-in electric field sweeps carriers quickly through the depletion region to deliver a photocurrent $\left(J_n+J_{dr}+J_p\right)$. Then we can get the internal quantum efficiency equation:

$$IQE(\lambda)=\left(IQE_n+IQE_{dr}+IQE_p\right)=\frac{J_{sc}(\lambda)}{qF(\lambda)}\cdot P=\frac{J_n(\lambda)+J_{dr}(\lambda)+J_p(\lambda)}{qF(\lambda)}\cdot P$$

$$IQE_{dr}=P\cdot[1-\mathrm{R}(\lambda)]\cdot exp\left(-\alpha_{cap}z_{cap}-\alpha_p\left(z_p-w_p\right)\right)\cdot\left(1-exp\left(-\alpha_p w_p-\alpha_i z_i-\alpha_n w_n\right)\right)$$

$$IQE_n=-\frac{P\cdot\alpha(\lambda,z)\cdot[1-R(\lambda)]\cdot l_n\cdot exp\left(-\alpha_{cap}z_{cap}\right)}{\alpha_p^2 l_n^2-1}\cdot\left[\frac{\alpha_p D_n+S_n}{B_n}-\frac{exp\left(-\alpha_p\left(z_p-w_p\right)\right)\cdot N_n}{B_n}-l_n\cdot\alpha_p\cdot exp\left(-\alpha_p\left(z_p-w_p\right)\right)\right]$$

$$IQE_p=-\frac{P\cdot\alpha(\lambda,z)\cdot[1-R(\lambda)]\cdot l_p\cdot exp\left(-\alpha_{cap}z_{cap}-\alpha_p z_p-\alpha_i z_i\right)}{\alpha_n^2 l_p^2-1}\cdot\left[\frac{\left(\alpha_n D_p+S_p\right)\cdot exp\left(-\alpha_n(\ z_n+z_i+z_p)\right)}{B_p}-\frac{exp\left(-\alpha_n(\ z_n+z_i+w_n)\right)\cdot N_p}{B_p}-l_p\cdot\alpha_n\cdot exp\left(-\alpha_n(\ z_n+z_i+w_n)\right)\right]$$

where the constant coefficients are:

$$B_n = \frac{D_n}{l_n} cosh \frac{z_p - w_p}{l_n} + S_n sinh \frac{z_p - w_p}{l_n}$$
$$N_n = \frac{D_n}{l_n} sinh \frac{z_p - w_p}{l_n} + S_n cosh \frac{z_p - w_p}{l_n}$$
$$B_p = \frac{D_p}{l_p} cosh - \frac{z_n - w_n}{l_p} + S_p sinh - \frac{z_n - w_n}{l_p}$$
$$N_p = \frac{D_p}{l_p} sinh - \frac{z_n - w_n}{l_p} + S_p cosh - \frac{z_n - w_n}{l_p}$$

Here, transport factor P represents the mean probability of an electron or hole crossing the intrinsic region without recombining. The calculation required transport properties of the cell materials and material parameters can be found in related reported literature.

3. Theoretical Results

We present the results for a Bi containing highly HMA GaBiAs QW p-i-n solar cells and vary the Bi composition to analyse the trends of optical and electronic properties and also to compare with the recently published experimental results on such a range of samples [16]. We calculate the IQE by using the models above with a selection of structures with different design values to study the influence on IQE of the following factors: induced Bi composition x (1% to 7% with 1% per step), the broadening linewidth δ (25 meV and 6.6 meV) and the number of QWs. The basic structure used here is the one illustrated schematically in Fig.1. In this example sample, light is coming through the optical cap (window) layer which is GaAs in this work, then we have a 600 nm $Al_{0.3}Ga_{0.7}As$ p-type layer and 620 nm undoped active layer with $GaBi_xAs_{1-x}$/GaAs QWs, and then 200 nm $Al_{0.3}Ga_{0.7}As$ n-type cladding layer and 200 nm n-type GaAs buffer layer, and GaAs n-type substrates beneath. All other material parameters are nearly well known and can be found from previous experimental studies reported in the related literature. We use the 12-band $k \cdot p$ model to calculate the band structure of $GaBi_xAs_{1-x}$ QWs solar cell, and then compute the optical elements by directly using the calculated QW eigenstates before [15]. The absorption coefficient is shown in Fig.2, [16].

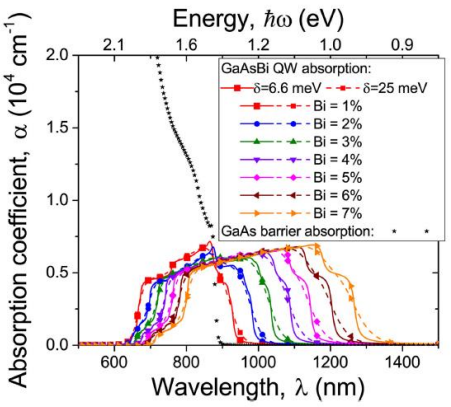


Fig. 2: The absorption spectrum used in the theoretical IQE. The absorption coefficient is consisted by two parts: (i) the $GaBi_xAs_{1-x}$ quantum well absorption efficiency is calculated using the 12-band $k \cdot p$ method with different Bi composition: from 1% to 7% per % per step, and broadening linewidth 6.6 meV and 25 meV (showing by solid and dashed lines, respectively); (ii) the GaAs bulk absorption efficiency (showing by black starts).

It is clearly to see in Fig.2 that there is quite a broad spectrum in the quantum well part of the absorption coefficient compared to the conventional III-V semiconductor alloys. The large inhomogeneous broadening occurs due to the impact of Bi-related alloy disorder on the VBE states. It can be find that the inhomogeneous broadening is large in magnitude and relatively independent of Bi composition, at least up to 7%. A distinct sharp peak can be observed in the absorption spectrum at low Bi composition, but it disappeared when increasing the composition of incorporated Bi. So that the impurity-like Bi atoms can broaden off the abrupt absorption. Meanwhile, the broad band edge of the optical spectrum move towards to the longer wavelength (small energy) with the increasing Bi composition. The strong absorption showing by black starts at short wavelength is from GaAs barrier material.

Then we used the calculated absorption coefficient as an input to the calculations of the IQE model with the design values of the example sample. We set the surface recombination velocity at $5 \times 10^4\ m/s$, and pick the electron escape probability P at surface of unity. We model the IQE in two groups for comparison, one series with 5 quantum wells in the i-region and other series with 40 QWs, and both of their $GaBi_xAs_{1-x}$ QWs are evenly spaced, have nominally 8 nm thick, but with different corresponding GaAs barriers thickness in order to maintain the same total thickness of i-regions. In both case, the IQE spectrum is generated with: (i) two different broadening linewidth of $\delta = 25\ meV$, specially for Bi-contained alloys, and $\delta = 6.6\ meV$, usually for conventional III-V alloys; (ii) seven different Bi composition, from 1% to 7%. Fig.3 (a) and (b) show the effects of Bi on IQE in $GaBi_xAs_{1-x}$.

As a test of our model and a comparison of our investigation about dilute bismide alloys. We also calculate the internal quantum efficiency of the conventional material InGaAs/GaAs QWs solar cells with the same design values of our Bi example sample. We choose the band gap of the test sample InGaAs/GaAs equal to that of Bi-contained sample with 4% Bi incorporated. So that the calculations have done on an 8 nm thick InGaAs QW and the same designed values as $GaBi_xAs_{1-x}$ to have a 1.15 eV band gap. And we also broaden the IQE of InGaAs/GaAs QWs with two broadening linewidth which is shown in Fig.3 (c).

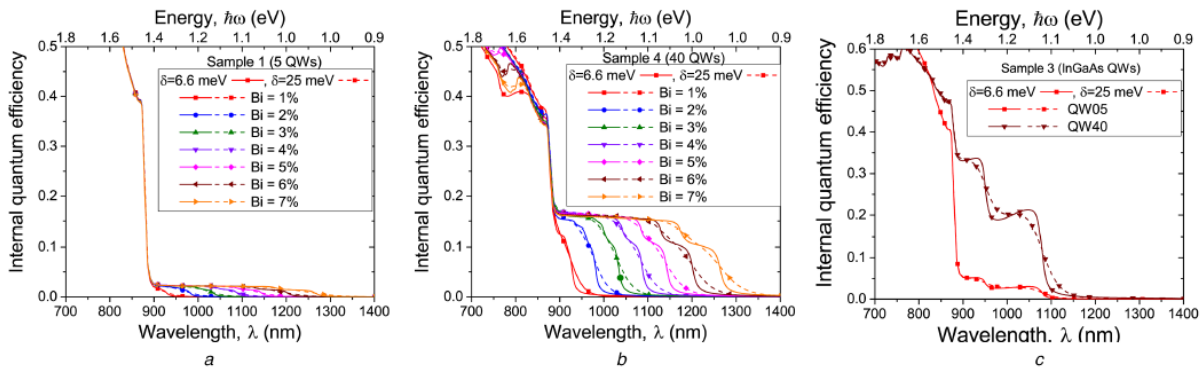


Fig. 3: The internal quantum efficiency spectrum of the example sample. (a) shows the results of sample 1 with 5 QWs in the model, (b) includes 40 QWs in the i-region. Dashed lines: $\delta = 25\ meV$, and Solid lines: $\delta = 6.6\ meV$. IQE spectrums calculated with Bi composition varied from 1% to 7% are shown with red, blue, green, purple, pink, wine and orange lines, respectively. (c) shows the IQE of InGaAs/GaAs QWs solar cells with 6.6 meV and 25 meV broadening linewidth, and 5 and 40 QWs for comparison.

The spectra clearly show that: (i) the inhomogeneous caused by the Bi-related atoms is large in magnitude compared to the IQE spectra in conventional semiconductor alloys such as InGaAs; and (ii) that the magnitude of the inhomogeneous broadening is relatively independent of Bi composition; (iii) more QWs means higher IQE in the longer wavelength, but we can see a small drop at the short wavelength which is because of less absorption by the substrate material when more photons are absorbed in the QWs region; (iv) the smaller broadening linewidth gives a much sharper band edges than the larger one. By comparing these calculations to experiment we found the broadening linewidth of 25 meV can well describe broad band edge features in GaBiAs alloys to the impact of Bi-induced alloy disorder [17]; (v) increasing the Bi composition will not affect the magnitude of IQE but shift the IQE towards to the longer wavelength.

When comparing IQE of the dilute bismide alloy $GaBi_xAs_{q-x}$ with the conventional material InGaAs/GaAs, we can easily find that the IQE is lower in this new material system. As we know, the magnitude of the internal quantum efficiency is directly corresponded to the magnitude of

the absorption coefficient at a given wavelength. And as we mentioned before, we calculate the absorption coefficient by directly using the eigenstates generated from the 12-band model. The 12-band $k \cdot p$ Hamiltonian includes the BAC interaction due to Bi incorporation which reduces the magnitude of the absorption spectrum [18].

4. Conclusion

We have introduced 10-, 12- and 14-band $k \cdot p$ models for the band structures of dilute nitride, bismide and bismide-nitride alloys, respectively. We have used this approach to model a dilute bismide QW alloy system in detail. The results of the band structure of dilute bismide alloys can be well described by using the BAC interaction between the highly localized Bi-related impurity-like resonant states and the extended GaAs VBE states.

We have also developed a general IQE approach to investigate using these HMA systems for photovoltaic applications and have used this model to study GaBiAs/GaAs QWs solar cells. We found that the GaBiAs/GaAs QW alloy system is a promising candidate to provide a suitable 1 eV junction for the development of highly efficient MJSCs. Our calculation suggests that we need a large number of QWs to have sufficiently high absorption and IQE at energies below the GaAs band gap. Therefore, we propose and are investigating the properties of some strain-balanced structures which will allow the growth of large numbers of QWs without suffering from strain-thickness limitations.

Acknowledgements: The authors thank colleagues at the Universities of Imperial College and Sheffield University for allowing us access to experimental results on the GaBiAs QW samples prior to publication. These results are now published in ref [19].

References

[1] C. A. Broderick, M. Usman, and E. P. O'Reilly, "Derivation of 12- and 14-band k · p Hamiltonians for dilute bismide and bismide-nitride semiconductors," *Semicond. Sci. Technol.*, vol. 28, p. 125025, 2013.

[2] J. Wu, W. Shan, and W. Walukiewicz, "Band anticrossing in highly mismatched III V semiconductor alloys," *Semicond. Sci. Technol.*, vol. 17, no. 8, pp. 860–869, 2002.

[3] J. A. Van Vechten and T. K. Bergstresser, "Electronic structures of semiconductor alloys," *Phys. Rev. B*, vol. 1, no. 8, pp. 3351–3358, 1970.

[4] M. Kondow, K. Uomi, K. Hosomi, and T. Mozume, “Gas-source molecular beam epitaxy of GaN/sub x/As/sub 1-x/ using a N radical as the N source,” *Japanese J. Appl. Phys. Part 2 Lett. Express Lett.*, vol. 33, no. 8A, pp. L1056-8, 1994.

[5] M. Kondow, K. Uomi, A. Niwa, T. Kitatani, S. Watahiki, and Y. Yazawa, “GaInNAs: A novel material for long-wavelength-range laser diodes with excellent high-temperature performance,” *Japanese J. Appl. Physics, Part 1 Regul. Pap. Short Notes Rev. Pap.*, vol. 35, no. 2 SUPPL. B, pp. 1273–1275, 1996.

[6] S. Tixier *et al.*, “Molecular beam epitaxy growth of GaAs1-xBix,” *Appl. Phys. Lett.*, vol. 82, no. 14, pp. 2245–2247, 2003.

[7] S. Francoeur, M.-J. Seong, A. Mascarenhas, S. Tixier, M. Adamcyk, and T. Tiedje, “Band gap of GaAs1−xBix, 0<x<3.6%,” *Appl. Phys. Lett.*, vol. 82, no. 22, pp. 3874–3876, 2003.

[8] K. Alberi *et al.*, “Valence-band anticrossing in mismatched III-V semiconductor alloys,” *Phys. Rev. B - Condens. Matter Mater. Phys.*, vol. 75, no. 4, pp. 1–6, 2007.

[9] W. Huang, K. Oe, G. Feng, and M. Yoshimoto, “Molecular-beam epitaxy and characteristics of GaNyAs1−x−yBix,” *J. Appl. Phys.*, vol. 98, no. 5, p. 53505, 2005.

[10] M. Usman, C. A. Broderick, A. Lindsay, and E. P. O’Reilly, “Tight-binding analysis of the electronic structure of dilute bismide alloys of GaP and GaAs,” *Phys. Rev. B - Condens. Matter Mater. Phys.*, vol. 84, no. 24, pp. 1–13, 2011.

[11] Z. Batool, K. Hild, T. J. C. Hosea, X. Lu, T. Tiedje, and S. J. Sweeney, “The electronic band structure of GaBiAs/GaAs layers: Influence of strain and band anti-crossing,” *J. Appl. Phys.*, vol. 111, no. 11, 2012.

[12] M. Paxman *et al.*, “Modeling the spectral response of the quantum well solar cell,” *J. Appl. Phys.*, vol. 74, no. 1, pp. 614–621, 1993.

[13] C. A. Broderick *et al.*, “Determination of type-I band offsets in GaBi x As 1– x quantum wells using polarisation-resolved photovoltage spectroscopy and 12-band k.p calculations,” *Semicond. Sci. Technol.*, vol. 30, p. 94009, 2015.

[14] K. Toprasertpong *et al.*, “Absorption threshold extended to 1.15 eV using InGaAs/GaAsP quantum wells for over-50%-efficient lattice-matched quad-junction solar cells,” *Prog. Photovoltaics Res. Appl.*, vol. 24, no. 4, pp. 533–542, Apr. 2016.

[15] I. P. Marko *et al.*, “Optical gain in GaAsBi/GaAs quantum well diode lasers,” *Sci. Rep.*, vol. 6, no. 1, p. 28863, 2016.

[16] R. D. Richards *et al.*, “Promise and challenges for GaAsBi as a photovoltaic material,” *Sol. Mater.*, p. 7, 2017 (accepted- in press).

[17] M. Usman *et al.*, “Impact of alloy disorder on the band structure of compressively strained GaBixAs1-x,” *Phys. Rev. B - Condens. Matter Mater. Phys.*, vol. 87, no. 11, pp. 1–10, 2013.

[18] C. A. Broderick, P. E. Harnedy, and E. P. O’Reilly, “Theory of the electronic and optical properties of dilute bismide Quantum Well Lasers,” *IEEE J. Sel. Top. Quantum Electron.*, vol. 21, no. 6, 2015.

[19] R. D. Richards *et al.*, “GaAsBi: An alternative to InGaAs based multiple quantum well photovoltaics,” *Conf. Rec. IEEE Photovolt. Spec. Conf.*, vol. 2016–Novem, no. Iv, pp. 1135–1137, 2016.